534,783

(12) INTERNATIONAL APPLICATION PUBLISHED UNDER THE PATENT COOPERATION TREATY (PCT)

(19) World Intellectual Property Organization
International Bureau

(43) International Publication Date
10 June 2004 (10.06.2004)

PCT

(10) International Publication Number
WO 2004/049008 A1

(51) International Patent Classification[7]: G01V 3/12

(21) International Application Number:
PCT/GB2003/005094

(22) International Filing Date:
24 November 2003 (24.11.2003)

(25) Filing Language: English

(26) Publication Language: English

(30) Priority Data:
0227451.2 25 November 2002 (25.11.2002) GB

(71) Applicant *(for all designated States except US)*: **OHM LIMITED** [GB/GB]; CEI (Building 37), University of Southampton, Highfield, Southampton, Hampshire SO17 1BJ (GB).

(72) Inventors; and

(75) Inventors/Applicants *(for US only)*: **MACGREGOR, Lucy, M.** [GB/GB]; 3 Montague Street, Edinburgh, EH8 9QT (GB). **SINHA, Martin, C.** [GB/GB]; 17 Radway Road, Upper Shirley, Southampton, SO15 7PN (GB). **WEANER, Richard** [GB/GB]; OHM Limited, CEI (Building 37), University of Southampton, Highfield, Southampton, Hampshire SO17 1BJ (GB).

(74) Agent: **D YOUNG & CO.**; 21 New Fetter Lane, London EC4A 1DA (GB).

(81) Designated States *(national)*: AE, AG, AL, AM, AT, AU, AZ, BA, BB, BG, BR, BY, BZ, CA, CH, CN, CO, CR, CU, CZ, DE, DK, DM, DZ, EC, EE, EG, ES, FI, GB, GD, GE, GH, GM, HR, HU, ID, IL, IN, IS, JP, KE, KG, KP, KR, KZ, LC, LK, LR, LS, LT, LU, LV, MA, MD, MG, MK, MN, MW, MX, MZ, NI, NO, NZ, OM, PG, PH, PL, PT, RO, RU, SC, SD, SE, SG, SK, SL, SY, TJ, TM, TN, TR, TT, TZ, UA, UG, US, UZ, VC, VN, YU, ZA, ZM, ZW.

(84) Designated States *(regional)*: ARIPO patent (BW, GH, GM, KE, LS, MW, MZ, SD, SL, SZ, TZ, UG, ZM, ZW), Eurasian patent (AM, AZ, BY, KG, KZ, MD, RU, TJ, TM), European patent (AT, BE, BG, CH, CY, CZ, DE, DK, EE, ES, FI, FR, GB, GR, HU, IE, IT, LU, MC, NL, PT, RO, SE, SI, SK, TR), OAPI patent (BF, BJ, CF, CG, CI, CM, GA, GN, GQ, GW, ML, MR, NE, SN, TD, TG).

Published:
— *with international search report*
— *before the expiration of the time limit for amending the claims and to be republished in the event of receipt of amendments*

[Continued on next page]

(54) Title: ELECTROMAGNETIC SURVEYING FOR HYDROCARBON RESERVOIRS

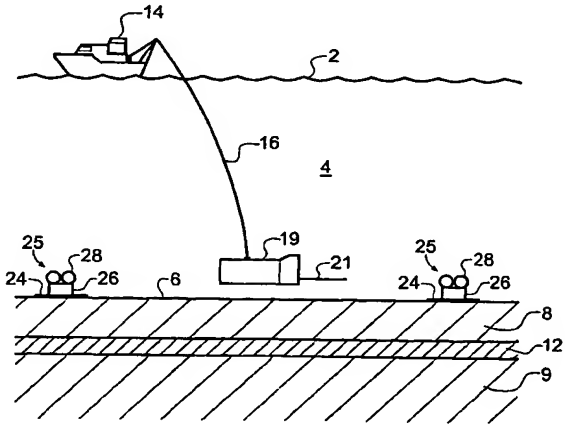

A

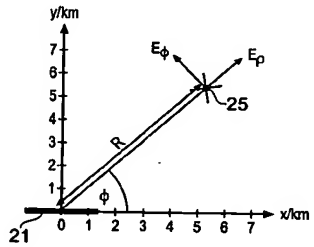

B

(57) Abstract: An electromagnetic survey method for surveying an area that potentially contains a subterranean hydrocarbon reservoir. The method comprises detecting a detector signal in response to a source electromagnetic signal, resolving the detector signal along at least two orthogonal directions, and comparing phase measurements of the detector signal resolved along these directions to look for a phase separation anomaly indicative of the presence of a buried hydrocarbon layer. The invention also relates to planning a survey using this method, and to analysis of survey data taken using this survey method. The first and second data sets may be obtained concurrently with a single horizontal electric dipole source antenna. The method is also largely independent of a source-detector pair's relative orientation and so provides for good spatial coverage and easy-to-perform surveying.

WO 2004/049008 A1

For two-letter codes and other abbreviations, refer to the "Guidance Notes on Codes and Abbreviations" appearing at the beginning of each regular issue of the PCT Gazette.

TITLE OF THE INVENTION

ELECTROMAGNETIC SURVEYING FOR HYDROCARBON RESERVOIRS

BACKGROUND OF THE INVENTION

The invention relates to seafloor electromagnetic (EM) surveying for oil and other hydrocarbon reserves.

Geophysical methods for mapping subterranean resistivity variations by various forms of EM surveying have been in use for many years [1, 2, 3, 10]. In these methods, electric field detectors are placed on the seafloor at carefully chosen positions at ranges up to about 10 km from an electromagnetic source. Detector signals measured at the detectors are sensitive to variations in subterranean strata configuration resistivity beneath the area being surveyed. However, EM surveying was not widely thought of as a technique that could be applied to finding hydrocarbon reservoirs.

More recently, it was proposed to use EM surveying to find hydrocarbon reservoirs. An early proposal by Statoil was to use the vertical current flow components to detect hydrocarbon layers [4, 5], since it is these components that are sensitive to the presence of a thin resistive layer. This was based on the understanding that a subterranean strata configuration that includes a resistive hydrocarbon layer embedded within less resistive sediments will give rise to a measurable enhancement of the electric field amplitude compared to a subterranean strata configuration comprising only water-bearing sediments. The Statoil proposal was to collect data from detector locations which are in-line with (i.e. end-on to) the axis of a horizontal electric dipole (HED) antenna so that the galvanic mode, that should be most sensitive to the presence of a buried high resistivity layer, dominates. However, it was established that the Statoil method could not provide reliable results, since the in-line data collected is incapable of distinguishing between a thin buried hydrocarbon layer of high resistivity situated in less resistive strata, on the one hand, and a non-hydrocarbon bearing rock formation in which the strata exhibits increasing resistivity

with depth, on the other hand, the latter being a common feature of many large scale sedimentary structures.

It was then proposed to use the EM surveying method according to Sinha [12] for finding hydrocarbon reservoirs [9, 13] and it was then confirmed that this method works well in practice for finding hydrocarbon reservoirs [6, 7]. The essence of the Sinha method is to normalise the in-line data with equivalent data for the same source-detector pair locations collected in an orthogonal geometry where the inductive mode dominates the response, referred to as a broadside geometry. In the broadside geometry the axis of the HED dipole antenna of the source is perpendicular to a line between the detector and source. EM surveying of a hydrocarbon reservoir applying the Sinha method is now described in more detail.

Survey data is collected by using a surface vessel to tow a submersible vehicle carrying a HED antenna over a survey area. The HED antenna broadcasts a source electromagnetic signal into the seawater. Detectors are located on the seafloor over the survey area and measure a signal in response to EM fields induced by the HED antenna. The amplitude of the detector signals is sensitive to resistivity variations in the underlying strata configuration and this is used to determine the nature of the subsea structure. In order to successfully map subterranean resistivity variations, the orientation of the current flows induced by the source electromagnetic signal must be considered [6]. The response of seawater and subterranean strata to the source electromagnetic signal is different for horizontally and vertically flowing induced current components. For horizontally flowing current components, the coupling between the layers comprising the subterranean strata is largely inductive. This means the presence of a thin resistive layers (which is indicative of a hydrocarbon layer) does not significantly affect the detector signal at the seafloor since the large scale current flow pattern is not affected by the thin resistive layer. On the other hand, for vertical current flow components, the coupling between layers is largely galvanic (i.e. due to the direct transfer of charge). In these cases even a thin resistive layer strongly affects the detector signals at the seafloor since the large scale current flow pattern is interrupted by the resistive layer.

While it is the vertical components of induced current flow which are most sensitive to the presence of a thin resistive layer, sole reliance on these components for detecting a hydrocarbon layer is not possible without ambiguity. The effects on the amplitude signals at the detectors arising from the presence a thin resistive layer can be indistinguishable from the effects which arise from other realistic large scale subterranean strata configurations. In order to resolve these ambiguities, it is necessary to determine the response of the subterranean strata to both horizontal (i.e. inductively coupled) and vertical (i.e. vertically coupled) induced current flows [6].

An electromagnetic source such as a HED antenna generates both inductive and galvanic current flow modes, with the relative strength of each mode depending on source-detector geometry. At detector locations which are broadside to the HED antenna dipole axis, the inductive mode dominates the response. At detector locations which are in-line with the HED antenna dipole axis, the galvanic mode is stronger [6, 8, 9, 10]. Accordingly, the response of the subterranean strata to vertical induced current flows along a line between a source location and a detector location is determined by arranging the HED antenna to present an end-on orientation to a detector, and the response of the subterranean strata to horizontal induced current flows along the line between the source location and the detector location is determined by arranging the HED antenna to present a broadside orientation to the detector. Data from both geometric configurations is required.

It is therefore important when designing a practical EM survey for detecting buried hydrocarbon layers using known techniques to distinguish between source and detector configurations in which the coupling between layers is largely inductive due to horizontal currents (in which case the survey has little sensitivity to the presence of a thin resistive layer) and those in which the coupling between layers is largely galvanic due to vertical currents (in which case blocking of the passage of this current flow by a reservoir leads to a survey which is strongly sensitive to the presence of a thin resistive layer).

Figure 1 shows in plan view an example survey geometry according to the Sinha method. There are sixteen detectors 25, and these are laid out in a square grid on a section of seafloor 6 above a subterranean hydrocarbon reservoir 56. The

hydrocarbon reservoir 56 has a boundary indicated by a heavy line 58. The orientation of the hydrocarbon reservoir is indicated by the cardinal compass points (marked N, E, S and W for North, East, South and West respectively) indicated in the upper right of the figure. To perform a survey, a source such as a HED antenna, starts from location 'A' and is towed along a path indicated by the broken line 60 through location 'B' until it reaches location 'C', which marks the end of the survey path. As is evident, the tow path first covers four parallel paths aligned with the North-South direction to drive over the four "columns" of the detectors. This portion of the survey path moves from location 'A' to location 'B'. Starting from location 'B', the survey path then covers four paths aligned with the East-West direction which drive over the four "rows" of detectors. Each detector is thus passed over in two orthogonal directions. The survey is completed when the source reaches the location marked 'C'.

During the towing process, each of the detectors 25 presents several different orientation geometries with respect to the source. For example, when the source is directly above the detector position D1 and on the North-South aligned section of the tow path, the detectors at positions D5, D6 and D7 are at different ranges in an end-on position, the detectors at positions D2, D3 and D4 are at different ranges in a broadside position and the detector at positions D8 and D9 are midway between. However, when the source later passes over the detector position D1 when on the East-West aligned section of the tow path, the detectors at positions D5, D6 and D7 are now in a broadside position, and the detectors at position D2, D3 and D4 are in an end-on position. Thus, in the course of a survey, and in conjunction with the positional information of the source, data from the detectors can be used to provide details of the source electromagnetic signal transmission through the subterranean strata for a range of distances and orientations between source and detector. Each orientation provides varying galvanic and inductive contributions to the signal propagation. In this way the continuous towing of the source can provide a survey which samples over the extent of the subterranean reservoir.

The Sinha method has been demonstrated to provide good results in practice. However, it has some limitations.

Firstly, since the two modes cannot be easily separated there will generally be a level of cross-talk between them at a detector and this can lead to ambiguities in the results.

Secondly, in order to obtain survey data from both in-line and broadside geometries, the HED antenna needs to present two different orientations at each source location. This requires the surface vessel to make multiple passes over broadcast locations and can lead to long and complex tow path patterns.

Thirdly, the survey can only provide the best data possible at discrete source locations. This is because of the geometric requirements of a HED antenna survey which dictate that, at any point during the survey, data can only be optimally collected from those detectors to which the HED antenna is arranged either in-line or broadside. At other orientations, separation of the inductively and galvanically coupled signals becomes more difficult, and resulting data are less reliable. For instance, referring to the figure, when the HED antenna is at a point on the tow path directly above the detector marked D1 and on the North-South aligned section of the tow path, in-line data can only be collected from the detectors marked D5, D6 and D7, whilst broadside data can only be collected from the detectors marked D2, D3 and D4. The other detectors (for example those marked D8, D9 and D10) provide only marginally useful information at this point of the survey because of the complex mixing of the galvanically and inductively coupled modes. Furthermore, if, for example, the HED antenna is at the location identified by reference numeral 57 in the figure, which is on a North-South aligned section of the tow path, in-line data can be collected from the detectors marked D3, D8, D9 and D10, but broadside data cannot be collected from any of the detectors. Since both broadside and in-line data are required for optimal analysis, the best data possible with the square detector array shown in the figure can only be collected from points along the tow path where the source is directly above one of the detector locations.

In summary, with the Sinha method, the time during which good quality data can be collected represents only a small fraction of the overall time taken to perform a survey. Furthermore, in addition to the survey being time-inefficient, it is necessary to accurately follow a complex tow path which has to complement the detector layout,

and the detectors themselves must also be carefully accurately arranged. The difficulties in controlling both the position and the orientation of a towed source antenna, coupled with this need to accurately follow a particular tow path relative to the detector grid, is one of the major sources of error in surveys of these kind. The disadvantages associated with the survey constraints imposed by the Sinha method are the price to pay for resolving the ambiguities inherent in the Statoil method.

SUMMARY OF THE INVENTION

According to the invention there is provided an electromagnetic survey method for surveying an area that is thought or is known to contain a subterranean hydrocarbon reservoir, comprising: transmitting a source electromagnetic signal from a source location; detecting a detector signal at a detector location in response thereto; and obtaining survey data indicative of phase difference between first and second components of the detector signal resolved along first and second directions respectively.

By comparing phase measurements of different components of the detector signal, a phase separation anomaly can be detected which is sensitive to the presence of a hydrocarbon layer or reservoir within a subterranean strata configuration. The presence or not a phase separation anomaly, and hence the presence or not of a hydrocarbon layer, can be determined with a single source orientation. There is no need, as there is with known methods based on amplitude, for data to be collected with different source orientations. Accordingly, surveys can be performed more quickly and without needing to accurately control the source orientation. Furthermore, because of this insensitivity of a phase measurement to the relative source orientation, reliable data collection is not limited to specific source location and detector location geometries, as is the case when collecting in-line/broadside amplitude data, and a much less complex and geometrically restrained towpath can be employed to survey an extended area.

The first and second components can be any two of radial, vertical and azimuthal. The clearest phase anomaly appears to occur from the pairing of radial and azimuthal components. It is also possible to use all three components together, i.e. to have first, second and third components.

The first, second and, if used, third directions are preferably orthogonal, since by observing geometrically independent components of the detector signals, there is minimal cross-talk between the first and second data sets, and the sensitivity to the presence of a hydrocarbon reservoir is accordingly increased.

The source electromagnetic signal can be broadcast from an antenna mounted on a submersible vehicle, or from a static location, such as within a borehole, or from an oil or gas platform.

The source electromagnetic signal can be emitted at different frequencies to obtain survey data at a plurality of different frequencies. Moreover, the source electromagnetic signal can be emitted at a variety of frequencies, preferably between 0.01 Hz and 10 Hz. The method can be advantageously repeated over the same survey area using different frequencies of source electromagnetic signal. Lower frequencies are generally preferred. By probing the subterranean strata at a number of different frequencies of source electromagnetic signal, it is possible to obtain improved vertical resolution of structures within the subterranean strata configuration.

The source signal can be from a horizontal electric dipole. Such a signal can be provided using existing equipment, and also allows relatively simple inversion modelling.

The invention also provides a method of analysing results from an electromagnetic survey of an area that is thought or known to contain a subterranean hydrocarbon reservoir, comprising: providing survey data indicative of phase difference between first and second components of a detector signal resolved along first and second directions respectively; extracting the phase differences from the survey data; and determining a metric from the phase differences that is predictive of the presence or absence of hydrocarbon.

The phase differences can be extracted by rotationally transforming the survey data from an instrument frame to a source frame.

The invention also provides a computer program product bearing machine readable instructions for implementing the analysis method.

The invention further provides a method of planning an electromagnetic survey of an area that is thought or known to contain a subterranean hydrocarbon reservoir, comprising: creating a model of the area to be surveyed including a seafloor, a rock formation containing a postulated hydrocarbon reservoir beneath the seafloor, and a body of water above the seafloor; setting values for depth below the seafloor of

the postulated hydrocarbon reservoir and resistivity structure of the rock formation; and performing a simulation of an electromagnetic survey in the model to obtain from the model phase differences between first and second components of a detector signal resolved along first and second directions respectively.

Repeated simulations for a number of distances between a source and a detector and frequencies can be performed in order to allow optimum surveying conditions in terms of source-to-detector distance and frequency of EM signal for probing the hydrocarbon reservoir to be selected when performing an electromagnetic survey. The effects of differing detectors array configurations and source tow paths can also be modelled.

The invention also provides a computer program product bearing machine readable instructions for implementing the planning method.

BRIEF DESCRIPTION OF THE DRAWINGS

For a better understanding of the invention and to show how the same may be carried into effect reference is now made by way of example to the accompanying drawings in which:

Figure 1 is a schematic plan view showing an example survey geometry following prior art principles in which sixteen detectors are laid out on a section of seafloor above a subterranean reservoir;

Figure 2A shows in schematic vertical section a surface vessel undertaking an EM survey;

Figure 2B is a plan view detailing a polar coordinate system;

Figure 3 shows in schematic vertical section a model uniform background subterranean strata configuration;

Figure 4 shows in schematic vertical section a model hydrocarbon-layer subterranean strata configuration;

Figure 5A shows a graph plotting calculations of phases of different components of detector signals seen during a model electromagnetic survey of the subterranean strata configurations shown in Figures 3 and 4;

Figure 5B shows a graph plotting differences in the phases shown in Figure 5A;

Figure 6 shows in schematic vertical section a model of a non-hydrocarbon bearing subterranean strata configuration;

Figure 7 shows a graph plotting calculations of phases of different components of detector signals seen during a model electromagnetic survey of the subterranean strata configurations shown in Figures 3, 4 and 7;

Figure 8 shows a graph plotting differences in the phases shown in Figure 7;

Figure 9A is a schematic plan view showing an example survey geometry according to an embodiment of the present invention in which sixteen detectors are laid out on a section of seafloor above a subterranean reservoir;

Figure 9B compares the signal coverage of the prior art method and the method of the invention;

Figure 10 shows a graph plotting calculations of phases of different components of detector signals seen during a model electromagnetic survey of the subterranean strata configurations shown in Figures 4 at two different source electromagnetic signal frequencies;

Figures 11A and 11B show graphs plotting differences in the phases shown in Figure 10;

Figure 12A shows a graph plotting calculations of differences in phases between different components of detector signals seen during a model electromagnetic survey of several hydrocarbon-layer subterranean strata configurations with an electromagnetic source signal frequency of 0.5 Hz;

Figure 12B shows a graph plotting calculations of differences in phases between different components of detector signals seen during a model electromagnetic survey of several hydrocarbon-layer subterranean strata configurations with an electromagnetic source signal frequency of 0.25 Hz;

Figure 12C shows a graph plotting calculations of differences in phases between different components of detector signals seen during a model electromagnetic survey of several hydrocarbon-layer subterranean strata configurations with an electromagnetic source signal frequency of 1.0 Hz;

Figure 12D shows a graph plotting calculations of differences in phases between different components of detector signals seen during a model electromagnetic survey of several hydrocarbon-layer subterranean strata configurations with an electromagnetic source signal frequency of 2.0 Hz;

Figure 13A shows a graph plotting calculations of phases of different components of detector signals seen during a model electromagnetic survey of several uniform background subterranean strata configurations;

Figure 13B shows a graph plotting differences in the phases shown in Figure 13A;

Figure 14 shows a graph plotting calculations of maximum observed differences in phases between different components of detector signals seen during a model electromagnetic survey of a hydrocarbon-layer subterranean strata

configuration, as a function of hydrocarbon-layer resistivity, and for several electromagnetic source frequencies;

Figure 15A shows a graph plotting calculations of phases of different components of detector signals seen during a model electromagnetic survey of the subterranean strata configurations shown in Figures 3 and 4;

Figure 15B shows a graph plotting differences in the phases shown in Figure 15A;

Figure 16A shows a graph plotting calculations of phases of different components of detector signals seen during a model electromagnetic survey of the subterranean strata configurations shown in Figures 3 and 4; and

Figure 16B shows a graph plotting differences in the phases shown in Figure 16A;

DETAILED DESCRIPTION

A method of electromagnetic surveying for oil and other hydrocarbon reserves is described which does not require separate data acquisition of the response of a subterranean strata configuration to inductively and galvanically coupled modes. The new method can be performed using pre-existing survey equipment.

Figure 2A schematically shows a surface vessel 14 undertaking EM surveying of a subterranean strata configuration in a way that is suitable for collecting survey data for carrying out the invention. The subterranean strata configuration includes an overburden layer 8, an underburden layer 9 and a hydrocarbon layer (or reservoir) 12. The surface vessel 14 floats on the surface 2 of the seawater 4. A deep-towed submersible vehicle 19 carrying a HED antenna 21 is attached to the surface vessel 14 by an umbilical cable 16 providing an electrical, optical and mechanical connection between the deep-towed submersible vehicle 19 and the surface vessel 14. The HED antenna broadcasts a source electromagnetic signal into the seawater 4.

One or more remote detectors 25 are located on the seafloor 6. Each detector 25 includes an instrument packages 26, a detector antenna 24, a floatation device 28 and a ballast weight (not shown). The detector antenna 24 measures a detector signal in response to EM fields induced by the HED antenna in the vicinity of the detector 25, the amplitude of the detector signals is sensitive to resistivity variations in the underlying strata configuration. The instrument package 26 records the detector signals for later analysis. The detector antenna 24 in this example comprises two orthogonal dipole antennae arranged to detect first and second components of the electric field in a horizontal plane, i.e. one which is parallel to the seafloor 6.

The detectors record two (or three) orthogonal components of the seafloor electric field as raw data. The raw survey data are then analysed, after recovery of the detectors and transfer of the raw data into a suitable computer. Initially a spectral analysis is performed to remove the component of the signal which corresponds to source transmission, as is conventional. The survey data are then combined with source and receiver navigation data, again as is conventional. Then the survey data are processed to rotate the electric fields from an 'instrument' frame (i.e. components

parallel to the receiver dipoles of the detector) to the 'source' frame (i.e. radial and azimuthal components referenced to the source-receiver geometry). This is a new processing step specific to the present invention.

Figure 2B is a schematic plan view detailing a polar-coordinate system which is used to describe the principles of the new method. The origin of the coordinate system is positioned at the centre of the HED antenna shown in Figure 2A, and zero-azimuth is aligned parallel to the dipole axis of the HED antenna, as indicated in Figure 2B (the HED antenna in this Figure not drawn to scale). In Figure 2B, a single detector 25 is shown positioned at a range of R km from the origin, and at an azimuth of $\Phi°$. The orthogonal dipole antennae comprising the detector antenna 24 are arbitrarily oriented in the horizontal plane as indicated in the figure.

Since the phase difference from the source of electromagnetic radiation from a horizontal dipole source is an azimuthally symmetric subterranean strata configuration is largely independent of azimuth Φ, phase measurements recorded at the detector antenna 24 are largely independent of the azimuthal position of the detector 25 shown in Figure 2B. This allows phase data to be collected equally over a wider range of source-detector orientations than is possible with amplitude data, and any inaccuracies in the measurement of the azimuthal position of the detector in the coordinate system shown in Figure 2B have a lesser effect.

In the following examples, the two components of detected electric field, also known as detector signal, for which the phase is measured are a radial component and an azimuthal component. The radial component is that component of the electric field resolved along a direction parallel to a line connecting the source location and the detector location, and marked E_ρ in Figure 2B. The azimuthal component is that component of the electric field resolved along a direction perpendicular to a line connecting the source location and the detector location and in a horizontal plane, and marked E_Φ in Figure 2B. The components of the detected electric field along these directions is determined from the angular orientation of the orthogonal dipole antennae comprising the detector antenna 24 relative to the line joining the source location and the detector location. This can be easily determined using standard instrumentation, such as, for example, active or passive sonar to determine the relative

positions of the source location and the detector location, and a magnetic compass to determine the detector antenna orientation.

In order to show how the respective phases of two spatial components (e.g. radial ρ and azimuthal Φ components) of the electric field can be used to detect the presence of a subterranean hydrocarbon reservoir, numerical forward modelling of the kind described by Chave and Cox [11] is applied to different model subterranean strata configurations.

Figure 3 shows in schematic vertical section a model background subterranean strata configuration. The configuration comprises a section of seafloor 106 beneath a 10 km depth of seawater 104. The seawater has a resistivity of 0.31 Ωm. Beneath the seafloor 106 is a uniform half-space sedimentary structure with a resistivity of 1 Ωm, the low resistivity being primarily due to aqueous saturation of pore spaces. This background subterranean strata configuration extends uniformly downwards for an infinite extent. Also indicated in Figure 3 are a HED antenna 21, and a detector 25, such as those shown in Figure 2A. The distance between the HED antenna and the detector (i.e. the range) is R km. The azimuthal position of the detector relative to the orientation of the HED antenna is arbitrary due to the insensitivity of the phase component of the detected electric field signals to azimuth.

Figure 4 shows in schematic vertical section a model hydrocarbon-layer subterranean strata configuration. A section of seafloor 106 lies beneath a 10 km depth of seawater 104 which has a resistivity of 0.31 Ωm. The strata configuration beneath the seafloor 106 comprises a 1 km thick overburden layer 108, representing sediments, arranged above a hydrocarbon layer 112. The overburden layer 108 has a resistivity of 1 Ωm, again, primarily due to aqueous saturation of pore spaces. The hydrocarbon layer 112 is 0.1 km thick, and has a resistivity of 100 Ωm. The relatively high resistivity of the hydrocarbon layer is due to the presence of non-conducting hydrocarbon within pore spaces. Below the hydrocarbon layer 112 is a sedimentary underburden layer 109, which, as for the overburden layer, has a resistivity of 1 Ωm. The underburden layer extends downwardly for an effectively infinite extent. Accordingly, except for the presence or absence of the hydrocarbon layer 112, the

background subterranean strata configuration of Figure 3 and the hydrocarbon-layer subterranean strata configuration of Figure 4 are identical. A HED antenna 21 and a detector 25 are again shown as in Figure 3.

Figure 5A shows a graph plotting the modelled phase θ of the radial and azimuthal components of the detected electric field for both the background subterranean strata configuration and the hydrocarbon-layer subterranean strata configuration models shown in Figures 3 and 4 respectively as a function of range R. The phase is measured relative to a source electromagnetic signal transmitted by the HED antenna 21. In this example, the source electromagnetic signal is at a frequency of 0.5 Hz. The radial and azimuthal components of the detected electric field for the background subterranean strata configuration are marked θ_ρ^B and θ_Φ^B respectively and the corresponding components of the detected electric field for the hydrocarbon-layer subterranean strata configuration are marked θ_ρ^R and θ_Φ^R respectively. The results show that θ_ρ^B, θ_Φ^B, θ_ρ^R and θ_Φ^R all advance steadily in phase with increasing range R. However, it is also clear that the rate of phase advance is less for the hydrocarbon-layer subterranean strata configuration than for the background subterranean strata configuration. In the case of the background subterranean strata configuration, the phase of both the radial and azimuthal components advances at a rate of around 90° per km. In addition, at ranges beyond about 2 km, the azimuthal component θ_Φ^B consistently lags the radial component θ_ρ^B by around 25°. In the hydrocarbon-layer subterranean strata configuration, however, the behaviour is somewhat different. Beyond around 5 km, the azimuthal component θ_Φ^R again lags the radial component θ_ρ^R by around 25°, however the phase of both components advances at a rate of around only 10° per km. This is significantly lower than that seen with the background subterranean strata configuration. Furthermore, at ranges between around 2 km and 5 km, the difference in phase between azimuthal component θ_Φ^B and the radial component θ_ρ^R varies significantly. A phase separation anomaly is seen which varies from close to 0° phase difference between the radial and azimuthal components of detected electric field to a maximum of almost 60°.

Figure 5B shows a graph plotting, for both the radial and azimuthal components, the difference in phase θ^R-θ^B between the hydrocarbon-layer and

background subterranean strata configurations as a function of range R. The difference in the radial components is marked $\theta_\rho^R - \theta_\rho^B$, and the difference in azimuthal components is marked $\theta_\Phi^R - \theta_\Phi^R$. The different rates of phase advancement seen with the hydrocarbon-layer and background subterranean strata configurations is apparent in the negative gradient of the curves beyond around 3 km. The differing behaviour at mid ranges (between around 2 km and 5 km) is apparent from the separation of the curves over this range.

These differences in phase behaviour, namely the relatively slow advancement in phase of both radial and azimuthal components when a reservoir is present, and the strong range-limited variation in phase between the radial and azimuthal components seen at mid-ranges when the reservoir is present, provide two useful characteristics with which to determine the presence or absence of a hydrocarbon layer within an otherwise uniform background.

For the practical application of controlled source electromagnetic surveying to hydrocarbon exploration, it is necessary that other common subterranean strata configurations do not lead to a behaviour similar to that seen in the hydrocarbon-layer subterranean strata configuration model. In particular, it is important to be able to distinguish between subterranean strata configurations which include a thin hydrocarbon layer and non-hydrocarbon containing subterranean strata configurations that have increasing resistivity with depth.

Figure 6 shows in vertical section a highly schematic model of a non-hydrocarbon containing subterranean strata configuration. This subterranean strata configuration exhibits increasing resistivity with depth, which is a common feature of many large scale sedimentary structures. Due, for example, to increasing expulsion of conducting seawater with depth from rising overburden pressure. As with the background and hydrocarbon-layer subterranean strata configurations described above, in the non-hydrocarbon bearing subterranean strata configuration a section of seafloor 106 lies beneath a 10 km depth of seawater 104. The strata beneath the seafloor 106 comprise a series of sedimentary layers of increasing resistivity. A first layer 110 has a uniform resistivity of 1 Ωm and a thickness of 1 km. A second layer 113 has a uniform resistivity of 5 Ωm and a thickness of 1 km. A third layer 114 has a

uniform resistivity of 50 Ωm and a thickness of 1 km. Beneath the third layer 114 is a fourth layer 116 which has a resistivity of 100 Ωm and extends downwardly for an infinite extent. A HED antenna 21 and a detector 25 are again shown as in Figure 3.

Figure 7 shows a graph which is similar to and will be understood from the description of Figure 5A above, but which also includes modelled curves determined for the non-hydrocarbon bearing subterranean strata configuration. The modelled curves marked θ_ρ^B, θ_Φ^B, θ_ρ^R and θ_Φ^R are the same as those shown in Figure 5A. The curves marked θ_ρ^S and θ_Φ^S show the radial and azimuthal components of the detected electromagnetic field seen with the non-hydrocarbon bearing subterranean strata configuration.

The behaviour of the variation in phase of the detected electric field as a function of range beyond around 5 km is broadly similar for the hydrocarbon-layer subterranean strata configuration and the non-hydrocarbon bearing subterranean strata configuration. There are moderate differences in gradient between the models for the example shown, and in some circumstances this may allow the two subterranean strata configurations to be distinguished. (In other examples, the gradients are almost the same.) However, even if measurable, the value of the gradient is likely to be a fairly unreliable indicator of subterranean strata configuration in practice. This is because different absolute values of resistivity, for instance a more or less resistive hydrocarbon layer in the hydrocarbon-layer subterranean strata configuration, or a more rapidly increasing resistivity with depth in a non-hydrocarbon bearing subterranean strata configuration, are likely to lead to changes in the observed gradients and cause confusion between the two models.

However, at ranges between around 2 km and 5 km, there is nothing in the phase of the detected electric fields in response to the non-hydrocarbon bearing subterranean strata configuration which resembles the phase separation anomaly seen with the hydrocarbon-layer subterranean strata configuration. The phase behaviour seen with the non-hydrocarbon bearing subterranean strata configuration much more closely resembles that of the background subterranean strata configuration across this range. Accordingly, it is the phase separation anomaly (and not the gradient) which provides the most appropriate indicator of subterranean strata configuration.

Figure 8 shows a graph plotting the difference in the phase $\Delta\theta$ between the radial and azimuthal components of the detected electric field for the three model subterranean strata configurations described above as function of range R. The curve marked $\Delta\theta^B$ in Figure 8 represents the difference between the curves marked $\theta_\Phi{}^B$ and $\theta_\rho{}^B$ in Figure 7 (with negative values corresponding to the azimuthal component lagging the radial component). The curves marked $\Delta\theta^R$ and $\Delta\theta^S$ in Figure 8 correspondingly represent the differences between the curves marked $\theta_\Phi{}^R$ and $\theta_\rho{}^R$, and $\theta_\Phi{}^S$ and $\theta_\rho{}^S$ in Figure 7 respectively.

The phase separation anomaly seen with the hydrocarbon-layer subterranean strata configuration (curve marked $\Delta\theta^R$ in Figure 8) is apparent as a clear trough centred at a range of around 3.5 km. The magnitude of the phase separation anomaly at this point is almost 60°. This difference in phase between the radial and azimuthal components of the detected electric field is about 30° more negative than the largest difference seen with either the background or the non-hydrocarbon bearing subterranean strata configurations. With current technology, a phase differences between the radial and azimuthal components of the detected electric field of 10° can be clearly resolved. Accordingly, the presence or not of a trough similar to that seen in Figure 8 is easily detectable, and able to distinguish between a hydrocarbon-layer subterranean strata configuration of the type shown in Figure 3, and the model subterranean strata configurations shown in Figures 4 and 6.

By distributing a linear array of detectors along a section of seafloor, and at each one recording suitable raw data in response to a source electromagnetic signal broadcast by a horizontal electromagnetic dipole source, plots such as those shown in Figure 8 can be generated from the phase information obtained from the raw data. The results of these plots can then be used to indicate the type subterranean strata configuration beneath a line joining the source and the detectors. Unlike previous survey methods, this can be done using a single dipole source and without the need to collect multiple data sets corresponding to different orientations of the source.

By distributing a planar array of detectors on a section of seafloor, and at each one recording raw data in response to a source electromagnetic signal broadcast by a horizontal electromagnetic dipole source, plots such as those shown in Figure 8 can be

generated for a number of different directions once the phase information has been extracted from the raw data. Because of the insensitivity of phase to the azimuthal position of a detector with respect to the source dipole axis, the plots along each of the different directions achievable with a planar array of detectors can be obtained simultaneously, irrespective of the dipole source orientation. This allows a thorough two- or three-dimensional survey to be performed without even having to move the source. This contrasts to previous methods where a relatively long and complicated tow of the dipole source is required to utilise all of the detectors in a planar array, and then only with relatively low spatial sampling. Whilst all of the detectors in a planar array can be utilised without moving the source, in practical surveys employing the new method, it is likely that the source will nonetheless be moved, such as shown in Figure 2A. Each new source position provides an entire set of useful source-detector geometries, and so provides more comprehensive sampling of the subterranean strata configuration for a given number of detectors. In addition, by moving the source, surveys can be fully performed where the detectors are deployed over an area with a characteristic scale larger than the range of distances over which phase measurements can be reliably used to indicate the presence of a hydrocarbon layer.

Figure 9A shows in plan view an area of seafloor 6 to be surveyed and which is similar to that shown in the prior art Figure 1. There are sixteen detectors 25 for recording the phase components described above. The detector are laid out in a square grid above a subterranean reservoir 56. Other detector distributions could be used instead, such as other grid shapes, or distributions that are not in a simple grid. (The constraints on detector placement patterns imposed by the amplitude-based methods of both Statoil and Sinha are therefore lifted.) The subterranean reservoir 56 has a boundary indicated by a heavy line 58. The orientation of the subterranean reservoir is indicated by the cardinal compass points (marked N, E, S and W for North, East, South and West respectively) indicated in the upper right of the figure. To perform a survey using an embodiment of the new method, a source starts from location 'A' and is towed along a path indicated by the broken line 120 to location 'B', which marks the end of the survey path. At most points along the tow path, useful data can be collected from all of the detectors. For example, when the source antenna is at the

location marked by the reference numeral 57 in Figure 9A, all sixteen of the detectors 25 are able to collect reliable data. This contrasts to the correspondingly similar location shown in Figure 1, again marked by the reference numeral 57, at which point no useful data can be collected using previous methods. Accordingly, the tow path shown in Figure 9A, which is startlingly simple compared to that shown in Figure 1, actually provides a much greater amount of valid data. As noted above, with the new method, it is only necessary to know the relative positions of the source and detectors, and the orientation of each detector antenna such that the radial and azimuthal components of the detected electric field can be geometrically resolved. Since the orientation of the antenna is not critical, there is no need for the tow path 120 shown in Figure 9A to closely follow a pattern defined by the grid of detectors. In fact, it is preferable for the tow path to not align too closely with the north-south and east-west based detector grid, since for detectors in an end-on position (i.e. at an azimuth of 0° in the coordinate system shown in Figure 2B), the amplitude of the azimuthal component of the detected electric field will be small for a dipole source, and the phase of this component more difficult to accurately establish. In source-detector orientations where either the radial or azimuthal components of the detected electric field are small, other components of the detected electric field may be employed, for instance as described further below.

Figure 9B is a graphical representation comparing the signal spread of the new phase method to the old inline/broadside amplitude method. The example reservoir 56 bounded by the perimeter 58 is shown. The dipole source is at an arbitrary location 57 within the reservoir with the HED antenna axis aligned W-E. In the old method, good quality inline amplitude data is only collectable within a narrow angular range 64 indicated by W-E dark shading in the figure, and good quality broadside amplitude data is only collectable within a narrow angular range 62 indicated by the N-S dark shading in the figure. The angular ranges 62 and 64 need to be narrow to ensure that one of the inductive and galvanic signal components dominates over the other. Data collected by detectors in the four main quadrants 66 is essentially bad data to be rejected from analysis. On the other hand, in the new method, the situation is reversed. The broad quadrants 66 become the regions over which good quality data is collected,

since they are the regions in which phase can be fully decomposed into the radial and azimuthal signal components needed for the phase-difference anomaly measurement, whereas the dark areas 62, 64 are angular areas where the collected data becomes unreliable since the magnitude of one of the radial and azimuthal signal components is likely to become too small causing signal-to-noise problems.

The modelled phase responses shown in Figures 5A, 5B, 7 and 8 were all calculated for a horizontal electromagnetic dipole source transmitting a source electromagnetic signal at a frequency of 0.5 Hz.

Figure 10 shows a graph plotting the modelled phase θ of the radial and azimuthal components of the detected electric field for the hydrocarbon-layer subterranean strata configuration model shown in Figures 3 as a function of R for two different frequencies of source electromagnetic signal. The modelled radial and azimuthal components of the detected electric field seen in response to a dipole source transmitting at a frequency of 2 Hz are marked θ_ρ^{2Hz} and θ_Φ^{2Hz} respectively, and the modelled radial and azimuthal components of the detected electric field seen in response to a dipole source transmitting at a frequency of 0.25 Hz are marked $\theta_\rho^{0.25Hz}$ and $\theta_\Phi^{0.25Hz}$ respectively. These curves, and also comparison with the modelled radial and azimuthal components of the detected electric field seen in response to a dipole source transmitting at a frequency of 0.5 Hz, marked θ_ρ^R and θ_Φ^R in Figure 5A, indicate a frequency dependence to the characteristics of the phase separation anomaly indicative of a buried hydrocarbon layer. Towards higher frequencies, the phases of the radial and azimuthal components advance faster than at lower frequencies, and the scale over which the phase separation anomaly characteristic of a hydrocarbon layer's presence occurs is also seen to be frequency dependent.

Figure 11A shows a graph plotting the difference in the phase $\Delta\theta$ between the radial and azimuthal components of the detected electric field for the reservoir and background model subterranean strata configurations described above as function of range R, in response to a dipole source transmitting at a frequency of 2 Hz. The curve marked $\Delta\theta^R$ in Figure 11A represents the difference between the curves marked θ_Φ^{2Hz} and θ_ρ^{2Hz} in Figure 10 (with positive values corresponding to the radial component

lagging the azimuthal component). The curve marked $\Delta\theta^B$ represents the corresponding data for the background model subterranean strata configuration.

Figure 11B is shows a graph plotting the difference in the phase $\Delta\theta$ between the radial and azimuthal components of the detected electric field for the reservoir and background model subterranean strata configurations described above as function of range R, in response to a dipole source transmitting at a frequency of 0.25 Hz. The curve marked $\Delta\theta^R$ in Figure 11B represents the difference between the curves marked $\theta_\Phi^{0.25Hz}$ and $\theta_\rho^{0.25Hz}$ in Figure 10 (with positive values corresponding to the radial component lagging the azimuthal component). The curve marked $\Delta\theta^B$ represents the corresponding data for the background model subterranean strata configuration.

It is clear from Figures 8, 11A and 11B, that the range over which the phase separation anomaly occurs is smaller at higher frequencies. At 2 Hz (see Figure 11A), the phase separation anomaly is centred at a range of around 3 km and occurs over a characteristic range of about 1 km. At 0.5 Hz (see Figure 8), the phase separation anomaly is centred at a range of around 3 km and occurs over a characteristic range of about 2 km. At 0.25 Hz (see Figure 11B), the phase separation anomaly is centred at a range of around 3 km and occurs over a characteristic range of about 3 km. For all frequencies, the maximum phase separation seen with the hydrocarbon-layer subterranean strata configuration is about 30° more negative than the phase difference that would be seen if the hydrocarbon layer were not present. This indicates that the presence of a hydrocarbon layer can be detected using a range of frequencies, each of which acts a probe of the subterranean strata configuration operating over a slightly different spatial scale.

Figure 12A is a graph showing the effect of differing overburden thicknesses. The graph plots the difference in the phase $\Delta\theta$ between the radial and azimuthal components of the detected electric field for several hydrocarbon-layer subterranean strata configurations with different overburden thicknesses as function of range R. In this example, the source electromagnetic signal is at a frequency 0.5 Hz. Curves are plotted for different hydrocarbon-layer subterranean strata configurations which, while otherwise similar to the hydrocarbon-layer subterranean strata configuration shown in Figure 4, have overburden thicknesses of 0.25 km, 0.5 km, 1.0 km, 1.5km and 2.5 km.

The curves corresponding to each different overburden thickness are correspondingly marked in the figure. The curve marked 1.0 in Figure 12A is identical to the curve marked $\Delta\theta^R$ in Figure 8 since the overburden thickness in the model shown in Figure 3 (and used for the modelling shown in Figure 8) is 1.0 km. The curve marked $\Delta\theta^B$ in Figure 12A is similar to and will be understood from the similarly marked curve in Figure 8. For each of the curves corresponding to different overburden thicknesses, the magnitude of the phase separation anomaly is roughly similar, varying from about 55° with an overburden thickness of 0.25 km to about 65° with an overburden thickness of 2.5 km. Accordingly, the method is equally able to detect a thin hydrocarbon layer at a range of depths beneath the sea floor. It is also apparent that the range at which the phase separation anomaly is maximum increases with increasing overburden thickness. This sensitivity of the range of maximum phase separation anomaly to overburden thickness can allow the depth of a reservoir to be determined with appropriate inversion modelling and suitable data coverage.

Figures 12B, 12C and 12D are similar to and will be understood from Figure 12A. However, Figures 12B, 12C and 12D show the response of different overburden thicknesses to different frequencies of source electromagnetic signal. Figure 12B shows the response to a source electromagnetic signal at a frequency 0.25 Hz, Figure 12C shows the response to a source electromagnetic signal at a frequency 1.0 Hz, Figure 12B shows the response to a source electromagnetic signal at a frequency 2 Hz. It can be seen that the phase separation anomaly is detectable with a range of frequencies over a range of overburden thicknesses. The magnitude of the phase separation anomaly is broadly similar at each of the different frequencies shown. As seen previously, the range over which the phase separation is apparent narrows with increasing frequency.

Figure 13A is a graph showing the effect of differing background resistivity. The graph plots the modelled phase θ of the radial and azimuthal components of the detected electric field for a background subterranean strata configuration similar to that shown in Figure 3, but with different resistivity values for the uniform subterranean strata, as a function of range R. In this example, the source electromagnetic signal is at a frequency 0.5 Hz. The phase of the radial and azimuthal

components of the detected electric field are calculated for resistivity values of 1 Ωm, 5 Ωm, 15 Ωm, 50 Ωm and 200 Ωm, as marked in the figure. For each resistivity value the phase of the radial component of the detected electromagnetic field is shown as a dashed line, and the phase of the azimuthal component is shown as a solid line. The pair of curves corresponding to the 1 Ωm resistivity value are identical to the curves marked θ_ρ^B and θ_Φ^B in Figure 5A. It is clear that the resistivity value for the subterranean strata in a uniform model containing no hydrocarbon reservoir has a significant effect on the detected phase. The rate of advancement of phase with range, for both the radial and azimuthal components of the detected electric field, falls with increasing background resistivity. For example, at a resistivity of around 15 Ωm, the rate of phase advancement with range is about 15° per km. This is similar to the rate of phase advancement seen with the reservoir subterranean strata configuration model and plotted in Figure 5A for ranges beyond around 5 km. This again demonstrates how absolute values of phase for each of the radial and azimuthal components can be an unreliable indicator of the likely presence of a hydrocarbon layer within an otherwise uniform resistivity background.

Figure 13B shows a graph plotting the difference in phase $\Delta\theta$ between the radial and azimuthal components of the detected electric field for each of the different resistivity value background subterranean strata configurations shown in Figure 13A. Each curve is appropriately marked according to the resistivity value of the model to which it corresponds. The curve marked 1 Ωm is identical to the curve marked $\Delta\theta^B$ in Figure 8. While the characteristic difference in phase for the radial and azimuthal components is depends on the resistivity of the uniform subterranean strata, none of the curves shown in Figure 13B display a range limited phase separation anomaly which, as seen in Figure 8, is indicative of the presence of a buried hydrocarbon layer. It is the resistivity contrast between a buried hydrocarbon layer and an otherwise uniform background which gives rise to the phase separation anomaly. Accordingly, by forming the phase difference between the radial and azimuthal components of the detected electric field in the manner described above, a hydrocarbon-layer containing subterranean strata configuration remains clearly distinguishable from a range of uniform subterranean strata configurations of differing resistivities.

Figure 14 is a graph showing the effect of hydrocarbon-layer resistivities. The graph plots the largest difference in phase max($\Delta\theta$) between the radial and azimuthal components of the detected electric field as a function of differing hydrocarbon-layer resistivity P, in a hydrocarbon-layer subterranean strata configuration which is otherwise similar to that shown in Figure 3. Curves are shown for source electromagnetic signal frequencies of 0.25 Hz, 0.5 Hz, 1 Hz and 2 Hz, as indicated in the figure. For example, with a source electromagnetic signal frequency of 0.5 Hz, and a hydrocarbon-layer resistivity of 100 Ωm, the largest difference in phase between the radial and azimuthal components of the detected electric field is about -58°. This particular value corresponds to the minimum seen in Figure 8 for the curve marked $\Delta\theta^R$. Typical hydrocarbon-layer resistivities are between a few tens of Ωm and a few hundreds of Ωm. It can be seen from Figure 14 that for all typical values of hydrocarbon-layer resistivity, a difference in phase between the radial and azimuthal components of the detected electric field of at least 30° is seen for all source electromagnetic signal frequencies. At lower frequencies, it is even higher.

This demonstrates that the above described method is able to detect hydrocarbon layers with different resistivities, and using a range of source electromagnetic signal frequencies.

It can also be seen from Figure 14 that the maximum phase difference between the radial and azimuthal components of the detected field is greatest for a hydrocarbon layer with a resistivity of about 50 Ωm. At resistivities above and below this value, a decreasing maximum phase difference is seen.

It has thus been demonstrated that the presence of a hydrocarbon layer in a subterranean strata configuration can be detected by observing the phase difference between radial and azimuthal components of detected electric field in response to a source electromagnetic signal from a horizontal electric dipole source. This has been shown to work over a wide range of source frequencies, for differing depths of burial of a hydrocarbon layer and for different subterranean strata configuration resistivity values.

Alternative Embodiments

Whilst in the above examples the radial and azimuthal components have been considered, similar techniques can also be employed using different components of the detected electromagnetic field. For instance, if the detectors 25 shown in Figure 2 were configured to also record the phase of the vertical component of the detected electric field (i.e. perpendicular to both the radial and azimuthal directions), the vertical component could be used in combination with another component to probe a subterranean strata configuration.

Figure 15A shows a graph plotting the modelled phase θ of the vertical and azimuthal components of the detected electric field for both the background subterranean strata configuration and the hydrocarbon layer subterranean strata configuration models shown in Figures 3 and 4 respectively as a function of R. The phase is measured relative to a source electromagnetic signal transmitted by the HED antenna. In this example, the source electromagnetic signal is at a frequency 0.5 Hz. The vertical and azimuthal components of the detected electric field for the background subterranean strata configuration are marked θ_z^B and θ_Φ^B respectively and the corresponding components of the detected electric field for the hydrocarbon-layer subterranean strata configuration are marked θ_z^R and θ_Φ^R respectively. Except for showing the vertical rather than the radial components of the detected electric field, this figure directly corresponds to Figure 5A.

Figure 15B shows a graph plotting the difference in the phase $\Delta\theta$ between the vertical and azimuthal components of the detected electric field for the two model subterranean strata configurations included in Figure 15A. The curve marked $\Delta\theta^B$ in Figure 15B represents the difference between the curves marked θ_Φ^B and θ_z^B in Figure 15A (with negative values corresponding to the vertical component lagging the azimuthal component). The curve marked $\Delta\theta^R$ Figure 15B correspondingly represents the difference between the curves marked θ_Φ^R and θ_z^R in Figure 15A.

Figure 16A shows a graph plotting the modelled phase θ of the vertical and radial components of the detected electric field for both the background subterranean strata configuration and the hydrocarbon-layer subterranean strata configuration models shown in Figures 3 and 4 respectively. The phase is measured relative to a

source electromagnetic signal transmitted by the HED antenna. In this example, the source electromagnetic signal is at a frequency 0.5 Hz. The vertical and radial components of the detected electric field for the background subterranean strata configuration are marked θ_z^B and θ_ρ^B respectively and the corresponding components of the detected electric field for the hydrocarbon-layer subterranean strata configuration are marked θ_z^R and θ_ρ^R respectively. Except for showing the vertical rather than the azimuthal components of the detected electric field, this figure directly corresponds to Figure 5A.

Figure 16B shows a graph plotting the difference in the phase $\Delta\theta$ between the vertical and radial components of the detected electric field for the two model subterranean strata configurations included in Figure 16A. The curve marked $\Delta\theta^B$ in Figure 16B represents the difference between the curves marked θ_ρ^B and θ_z^B in Figure 16A (with negative values corresponding to the vertical component lagging the radial component). The curve marked $\Delta\theta^R$ Figure 18B correspondingly represents the difference between the curves marked θ_ρ^R and θ_z^R in Figure 18A.

Figures 15B and 16B both indicate that the difference in phase between the vertical component of detected electric field and either of the azimuthal or radial components is also sensitive to the presence of a hydrocarbon layer in an otherwise uniform background subterranean strata configuration. The phase difference seen between the vertical and azimuthal components displays both a negative and a positive lobe compared to the background subterranean strata configuration with a crossover at a range of around 4 km. This would be particularly useful indicator for use in survey areas where background resistivity is poorly constrained. The qualitative behaviour of the phase of the vertical component of the detected electric field is approximately similar to that of the azimuthal component. However, a larger phase separation is seen when comparing the radial component with the azimuthal component than when comparing the radial component with the vertical component. Accordingly, the azimuthal component will generally be preferred when comparison is made with the radial component, unless, for instance, the magnitude of the azimuthal component is small, for example, where a detector is very close to an end-on orientation.

In the above description, and in Figures 5A, 7, 10, 13A, 15A and 15B, the absolute phase of various components of the detected electric field has been considered relative to the source electromagnetic signal phase. However, in practice, since it is the relative between different components of the detected electric field seen at the detector which is indicative of the presence of a hydrocarbon layer, the detected components may be directly compared without reference to the phase of the source electromagnetic signal.

Finally it will be understood that the invention is equally applicable to surveying of freshwater, for example large lakes, so that references to seafloor, seawater etc. should not be regarded as limiting.

Summary

It has been demonstrated how a phase separation anomaly occurs in response to a hydrocarbon layer which is not seen with a background subterranean strata configuration. This allows the detection of subterranean hydrocarbon reservoirs and hydrocarbon bearing layers. The technique has many advantages over previous methods, for example:

- Previous techniques based on comparison of amplitude measurements require the collection of both end-on and broadside data for each receiver to be reliable. This requires multiple orthogonal survey tow paths (see Figure 1). Using a technique such as described above, a survey may be completed more thoroughly with a much shorter and less complex tow path (see Figure 9A).
- The orthogonal towpaths required by previous methods lead to sampling of different parts of a target structure. Because only single source-receiver pairs are required for a phase-based detection of the reservoir, there is reduced interpretational ambiguity arising from the dimensionality of the target structure. This overcomes the limitation of the prior art Sinha method in which in-line data from a given receiver will come from one source position and the corresponding broadside data at the same range will generally come from a different source location. This means that the

structure sampled between the source and detector for the compared in-line and broadside data will not be the same. With the new method, this problem does not arise, since all the data is collected from a single source position, so both phase components in the processed signal are derived from sampling the same structure.

- The above described technique is almost independent of detector azimuth relative to a source's dipole axis. Since the method is less dependent on the orientation of the source, geometry-related errors are much reduced. In order to decompose the detector signals into radial and azimuthal (or whichever components are desired) it is only necessary to know the relative positions of the source and detectors, and the orientation of the detector antenna. These can be easily determined using existing technology.

- The phase separation seen above is range limited and can be controlled by varying the frequency of the electromagnetic source. If the source were to broadcast at several discrete frequencies (either by employing multiple source antenna or a tuned source for example) improved vertical resolution can be achieved.

- For a particular source dipole transmission frequency, the range dependence of phase separation can be used to indicate the depth to the resistive layer.

- Phase data are relatively insensitive to structures which are local to the receiver.

REFERENCES

[1] Sinha, M.C., Patel, P.D., Unsworth, M.J., Owen, T.R.E. & MacCormack, M.R.G. An active source electromagnetic sounding system for marine use. *Mar. Geophys. Res.*, **12**, 1990, 59-68.

[2] Evans, R. L., Sinha, M. C., Constable, S. C. & Unsworth, M. J. On the electrical nature of the axial melt zone at 13°N on the East Pacific Rise. *J. Geophys. Res.*, **99**, 1994, 577 – 588

[3] Edwards, R.N., Law, K.L., Wolfgram, P.A., Nobes, D.C., Bone, M.N., Trigg, D.F. & DeLaurier, J.M., First result of the MOSES experiment: Sea sediment conductivity and thickness determination, Bute Inlet, Columbia, bu magnetometric offshore electrical sounding, *Geophyics, 50, 1985, 153-161*

[4] WO 00/13046 A1

[5] WO 01/57555 A1

[6] Eidesmo, T., Ellingsrud, S., MacGregor, L.M., Constable, S., Sinha, M.C., Johansen, S, Kong, F-N & Westerdahl, H., Sea Bed Logging (SBL), a new method for remote and direct identification of hydrocarbon filled layers in deepwater areas, *First Break, 20, 2002, 144-152.*

[7] Ellingsrud, S., Sinha, M.C, Constable, S., MacGregor, L.M., Eidesmo, T. & Johansen, S., Remote sensing of hydrocarbon layers by sea-bed logging (SBL): Results from a cruise offshore Angola, *The Leading Edge, submitted 2002.*

[8] MacGregor, L. M. & Sinha, M.C. Use of marine controlled source electromagnetic sounding for sub-basalt exploration. *Geophysical Prospecting*, **48**, 2000, 1091-1106.

[9] WO 02/14906 A1

[10] MacGregor, L.M., Constable, S.C. & Sinha, M.C. The RAMESSES experiment III: Controlled source electromagnetic sounding of the Reykjanes Ridge at 57° 45' N. *Geophysical Journal International*, **135**, 1998, 773-789.

[11] Chave, A.D. & Cox, C.S., Controlled electromagnetic sources for measuring electrical conductivity beneath the oceans, 1. Forward problem and model study. *J. Geophys. Res.*, **87**, 1982, 5327 – 5338

[12] Martin C. Sinha, "Controlled source EM sounding: Survey design considerations for hydrocarbon applications", *LITHOS Science Report April 1999, 1, 95-101*

[13] GB 2382875 A

CLAIMS

1. An electromagnetic survey method for surveying an area that is thought or is known to contain a subterranean hydrocarbon reservoir, comprising:

transmitting a source electromagnetic signal from a source location;

detecting a detector signal at a detector location in response thereto; and

obtaining survey data indicative of phase difference between first and second components of the detector signal resolved along first and second directions respectively.

2. The survey method of claim 1, wherein the first and second components are radial and azimuthal.

3. The survey method of claim 1, wherein the first and second components are vertical and azimuthal.

4. The survey method of claim 1, wherein the first and second components are vertical and radial.

5. The survey method of claim 1, further comprising obtaining survey data indicative of phase of a third component of the detector signal resolved along a third direction orthogonal to the first and second directions.

6. The survey method of claim 5, wherein the first and second and third components are vertical, radial and azimuthal.

7. The survey method of any one of the preceding claims, wherein the first and second directions are orthogonal.

8. The survey method of any one of claims 1 to 7, wherein the source electromagnetic signal is broadcast from an antenna mounted on a submersible vehicle which is towed over the survey area to move the source location.

9. The survey method of any one of claims 1 to 7, wherein the source location is fixed.

10. The survey method of any one of the preceding claims, wherein the source electromagnetic signal is emitted at different frequencies to obtain survey data at a plurality of different frequencies.

11. The survey method of any one of the preceding claims, wherein the source electromagnetic signal is emitted at a frequency of between 0.01 Hz and 10 Hz.

12. A method of analysing results from an electromagnetic survey of an area that is thought or known to contain a subterranean hydrocarbon reservoir, comprising:

providing survey data indicative of phase difference between first and second components of a detector signal resolved along first and second directions respectively.

extracting the phase differences from the survey data; and

determining a metric from the phase differences that is predictive of the presence or absence of hydrocarbon.

13. The analysis method of claim 12, wherein the first and second components are radial and azimuthal.

14. The analysis method of claim 12, wherein the first and second components are vertical and azimuthal.

15. The analysis method of claim 12, wherein the first and second components are vertical and radial.

16. The analysis method of claim 12, further comprising obtaining survey data indicative of phase of a third component of the detector signal resolved along a third direction orthogonal to the first and second directions.

17. The analysis method of claim 16, wherein the first and second and third components are vertical, radial and azimuthal.

18. The analysis method of any one of claims 12 to 17, wherein the first and second directions are orthogonal.

19. The analysis method of claim 18, wherein the phase differences are extracted by rotationally transforming the survey data from an instrument frame to a source frame.

20. A computer program product bearing machine readable instructions for implementing the method of any one of claims 12 to 19.

21. A method of planning an electromagnetic survey of an area that is thought or known to contain a subterranean hydrocarbon reservoir, comprising:

creating a model of the area to be surveyed including a seafloor, a rock formation containing a postulated hydrocarbon reservoir beneath the seafloor, and a body of water above the seafloor;

setting values for depth below the seafloor of the postulated hydrocarbon reservoir and resistivity structure of the rock formation; and

performing a simulation of an electromagnetic survey in the model to obtain from the model phase differences between first and second components of a detector signal resolved along first and second directions respectively.

22. The planning method of claim 21, wherein the first and second components are two of radial, vertical and azimuthal.

23. The planning method of claim 21 or 22, further comprising:

repeating the simulation for a number of distances between a source and a detector and frequencies in order to select optimum surveying conditions in terms of source-to-detector distance for probing the hydrocarbon reservoir.

24. A computer program product bearing machine readable instructions for implementing the planning method of claim 21, 22 or 23.

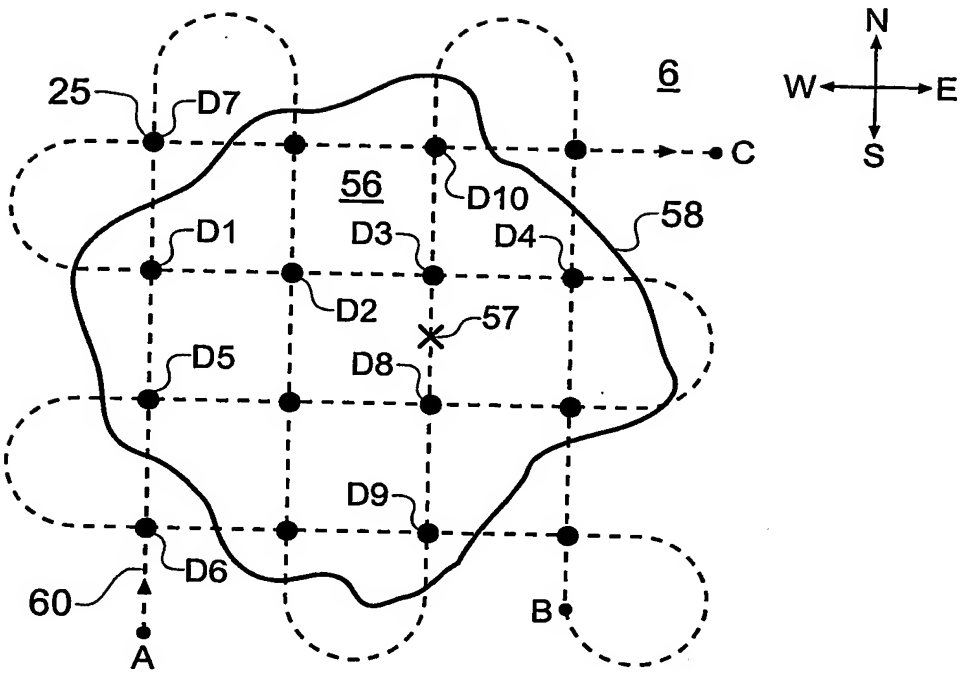

Fig. 1

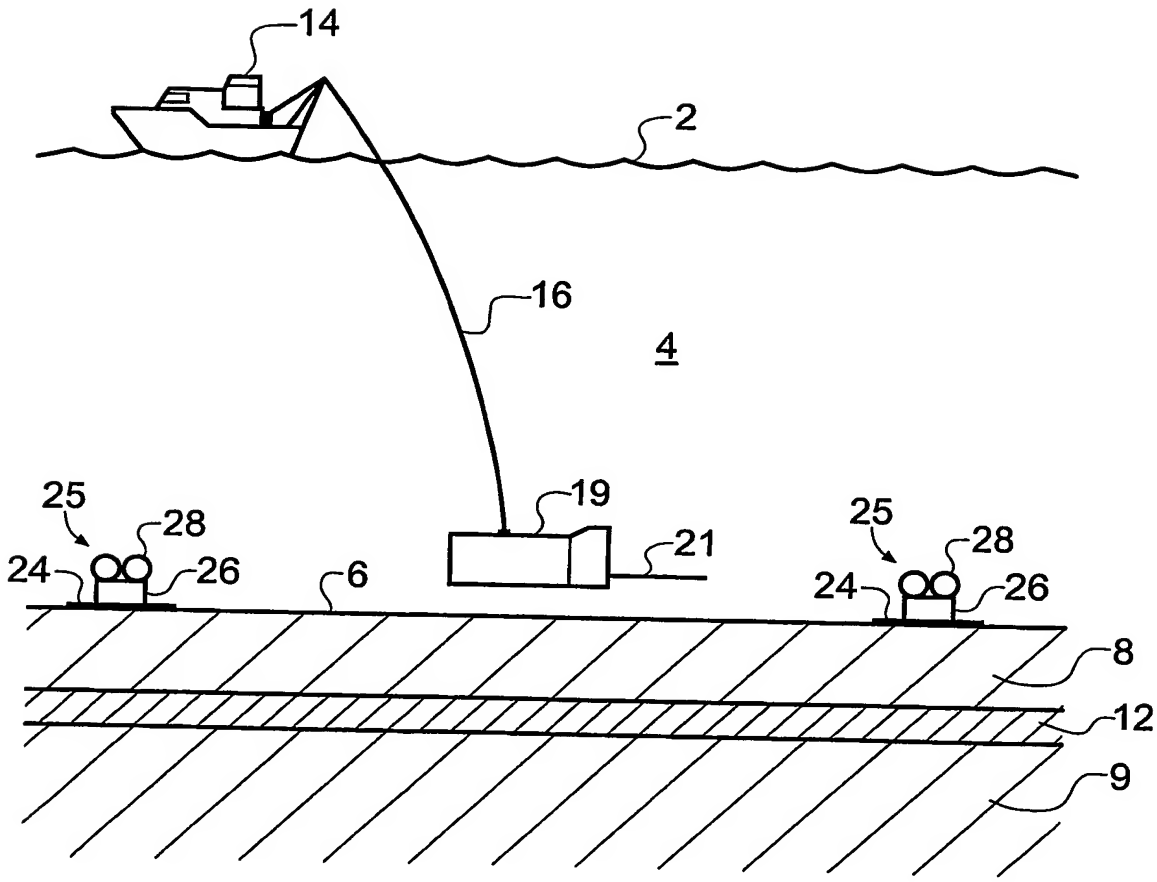

Fig. 2A

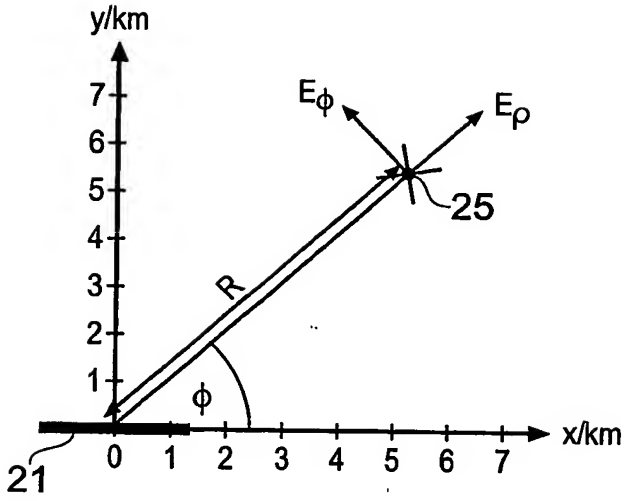

Fig. 2B

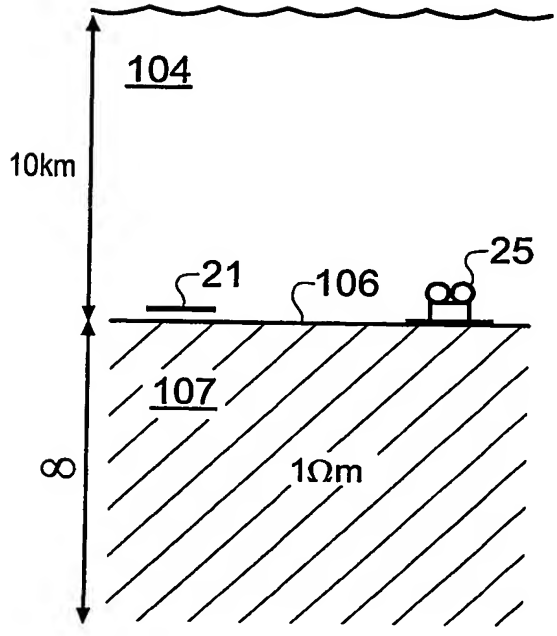

Fig. 3

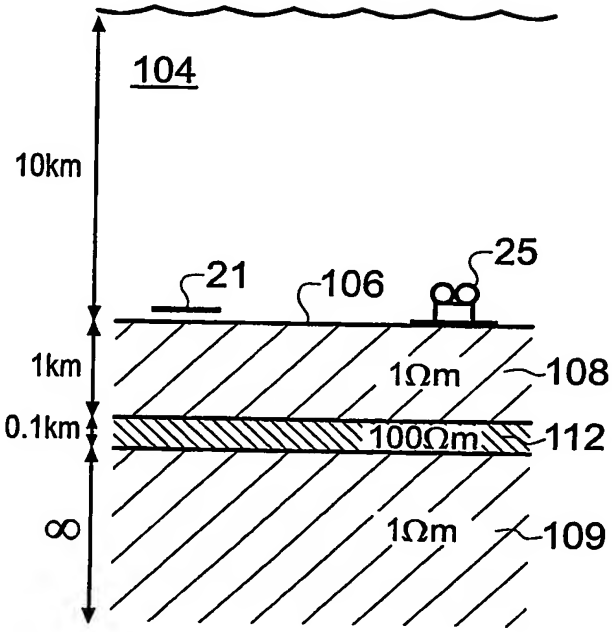

Fig. 4

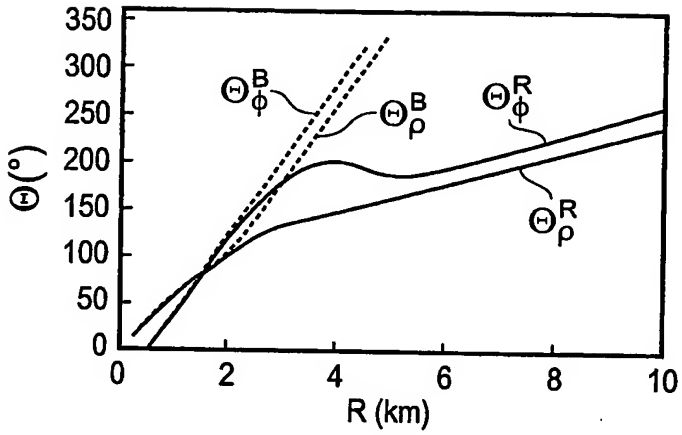

Fig. 5A

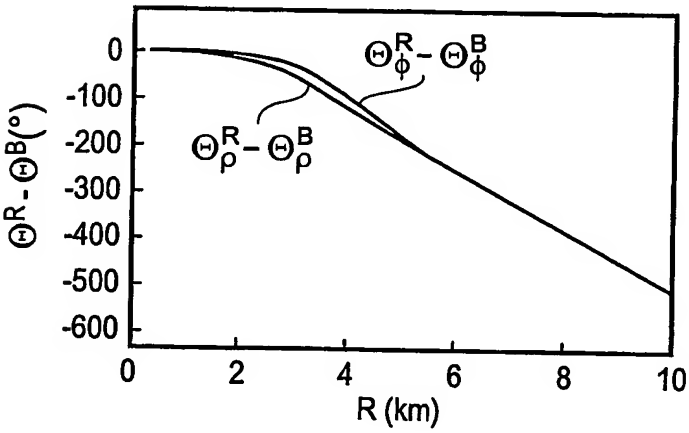

Fig. 5B

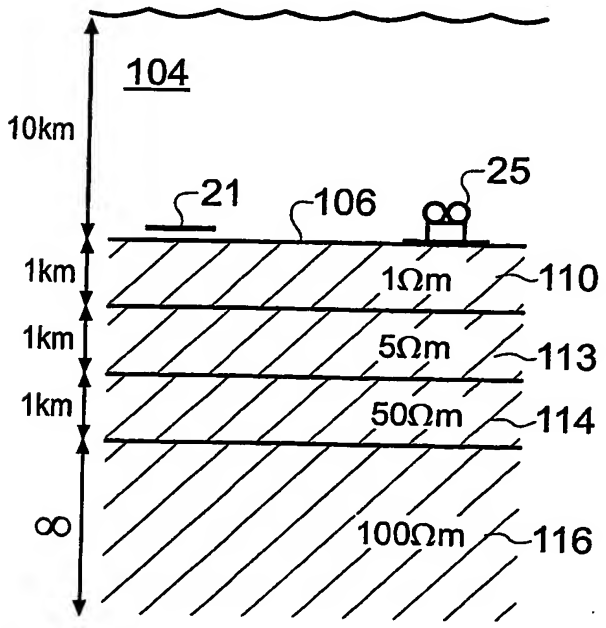

Fig. 6

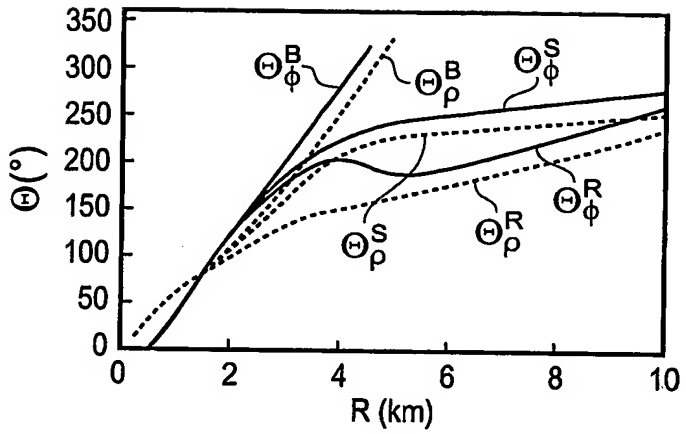
350
300
250
200
150
100
50
0
Θ(°)
0
2
4
6
8
10
R (km)
Θ_ϕ^B
Θ_ρ^B
Θ_ϕ^S
Θ_ρ^S
Θ_ρ^R
Θ_ϕ^R

Fig. 7

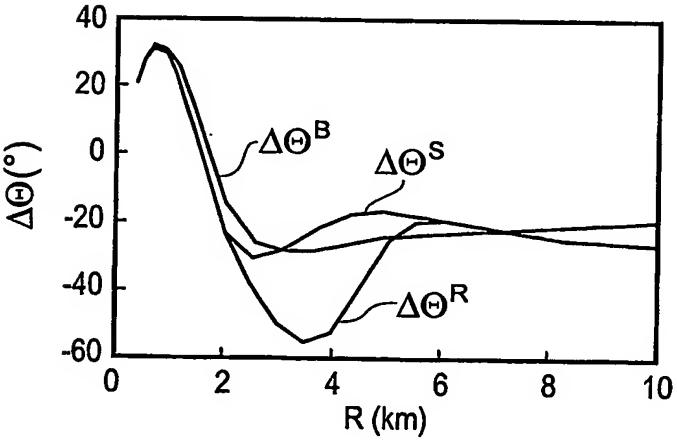
40
20
0
-20
-40
-60
ΔΘ(°)
0
2
4
6
8
10
R (km)
$\Delta\Theta^B$
$\Delta\Theta^S$
$\Delta\Theta^R$

Fig. 8

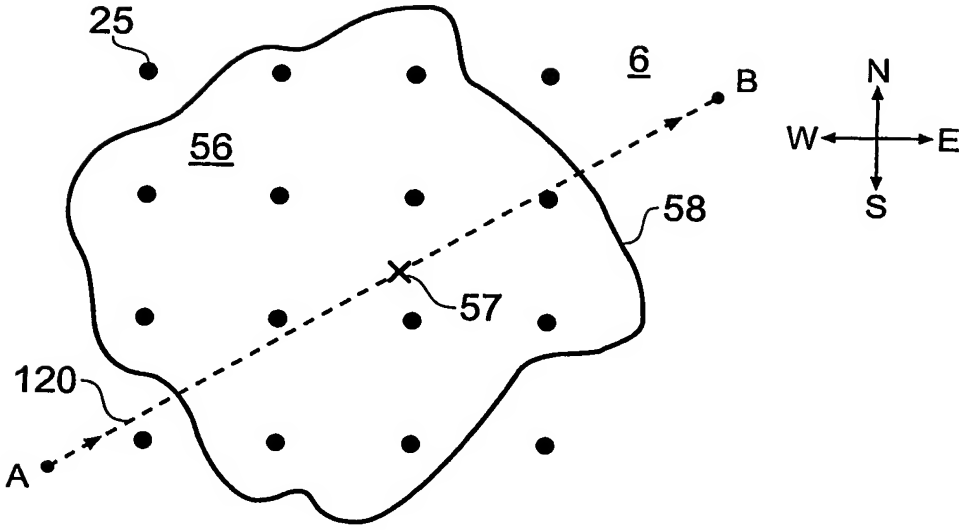

Fig. 9A

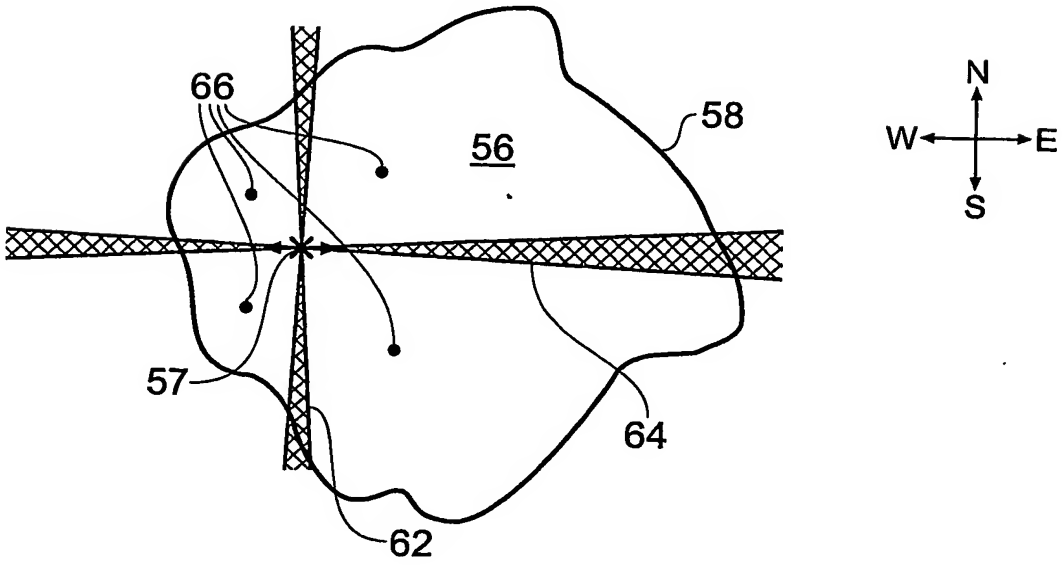

Fig. 9B

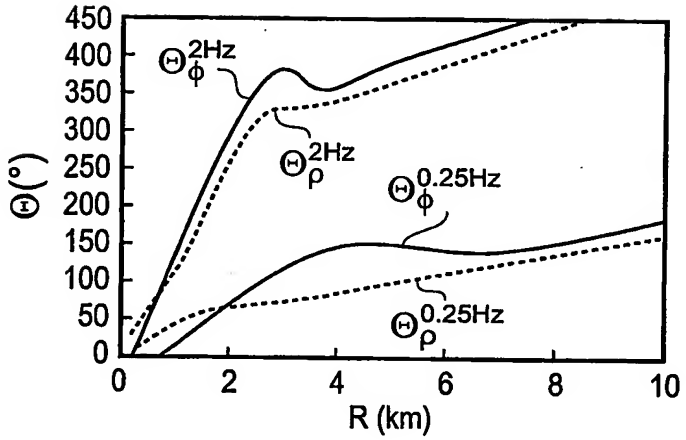

Fig. 10

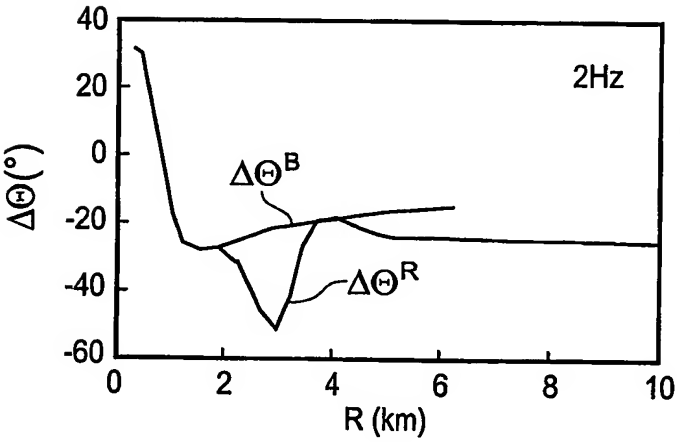

Fig. 11A

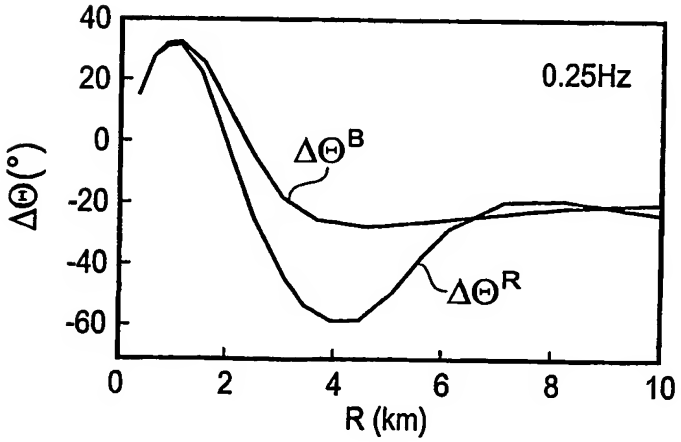

Fig. 11B

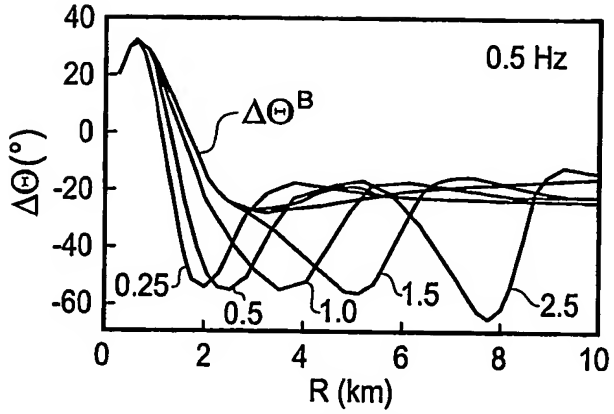

Fig. 12A

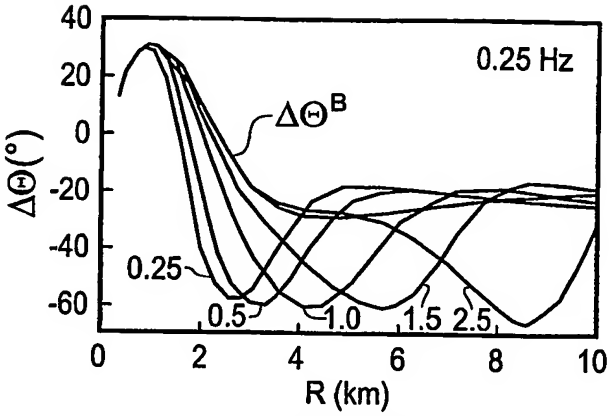

Fig. 12B

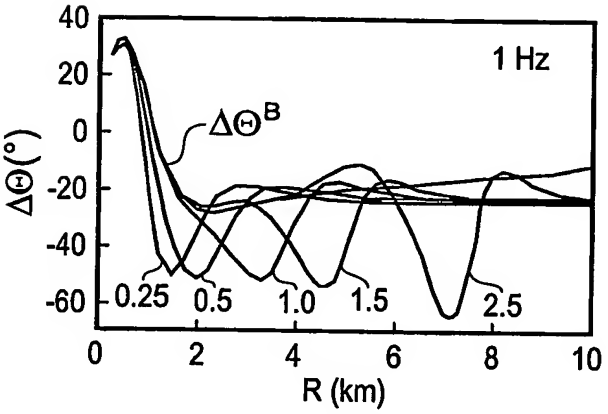

Fig. 12C

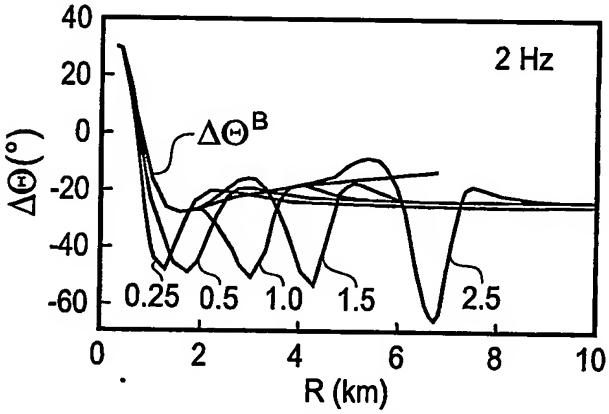

Fig. 12D

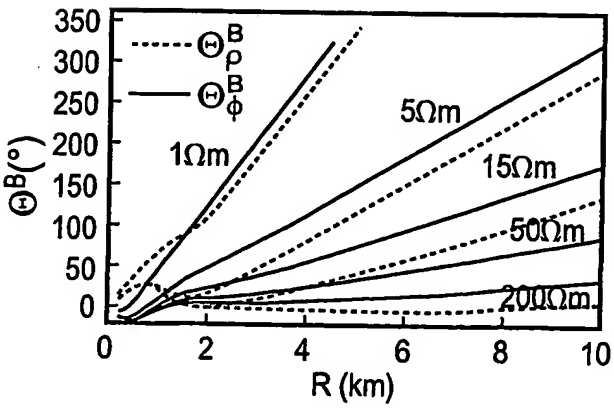

Fig. 13A

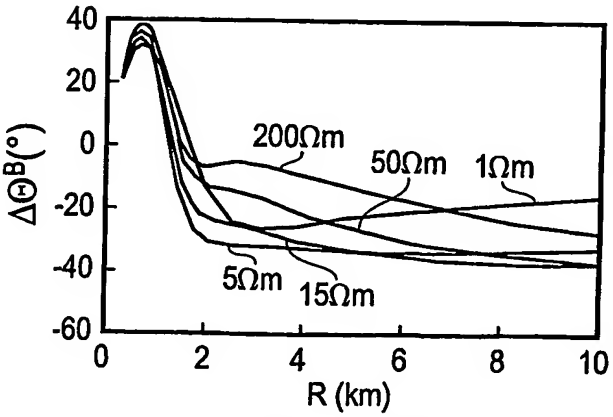

Fig. 13B

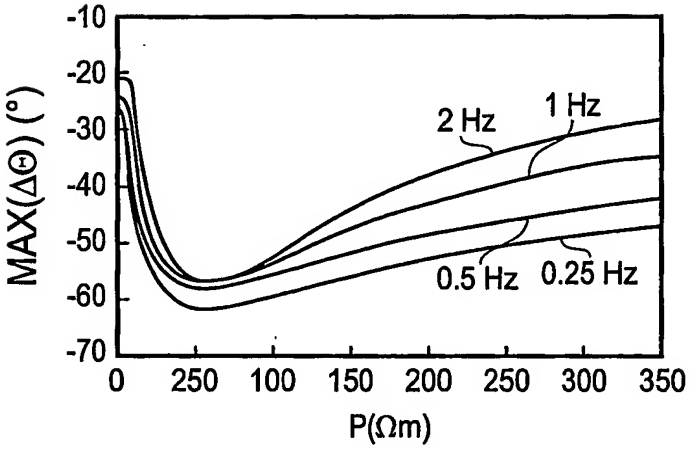
-10
-20
-30
-40
-50
-60
-70
MAX(ΔΘ) (°)
2 Hz
1 Hz
0.5 Hz
0.25 Hz
0
250
100
150
200
250
300
350
P(Ωm)

Fig. 14

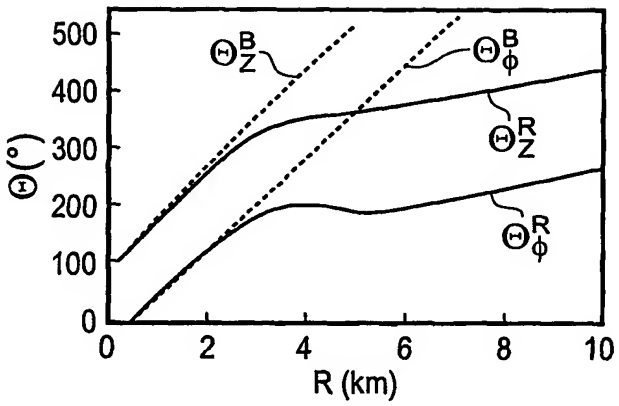

Fig. 15A

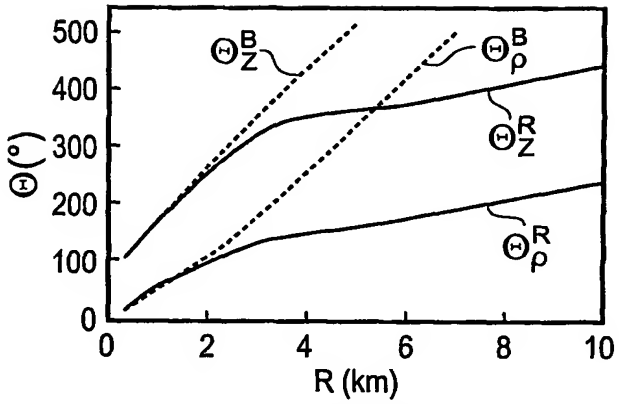

Fig. 16A

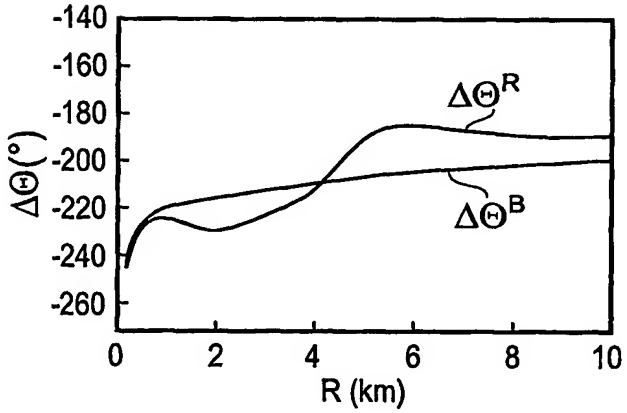

Fig. 15B

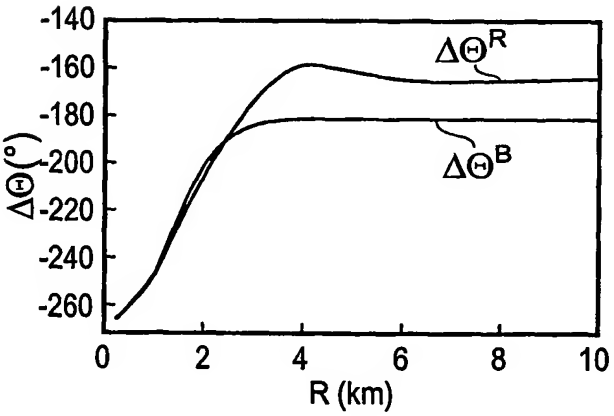

Fig. 16B

INTERNATIONAL SEARCH REPORT

PCT/GB 03/05094

A. CLASSIFICATION OF SUBJECT MATTER
IPC 7 G01V3/12

According to International Patent Classification (IPC) or to both national classification and IPC

B. FIELDS SEARCHED

Minimum documentation searched (classification system followed by classification symbols)
IPC 7 G01V

Documentation searched other than minimum documentation to the extent that such documents are included in the fields searched

Electronic data base consulted during the international search (name of data base and, where practical, search terms used)
EPO-Internal, WPI Data, INSPEC, COMPENDEX

C. DOCUMENTS CONSIDERED TO BE RELEVANT

Category °	Citation of document, with indication, where appropriate, of the relevant passages	Relevant to claim No.
X	WO 01/20366 A (EXXONMOBIL UPSTREAM RES CO) 22 March 2001 (2001-03-22) page 14, line 3 - line 2 page 24, line 11 - line 15	1,4,5,7, 9-11
Y		8,12,15, 16,18,20
P,X	GB 2 382 875 A (MACGREGOR LUCY MARGARET ; UNIV SOUTHAMPTON (GB)) 11 June 2003 (2003-06-11) cited in the application page 6, line 3 - line 8 page 16, line 10 - page 17, line 14	1-18, 20-24
Y	US 4 617 518 A (SRNKA LEONARD J) 14 October 1986 (1986-10-14) column 6, line 30 - line 35	8,12,15, 16,18,20
	-/--	

[X] Further documents are listed in the continuation of box C.

[X] Patent family members are listed in annex.

° Special categories of cited documents :

"A" document defining the general state of the art which is not considered to be of particular relevance

"E" earlier document but published on or after the international filing date

"L" document which may throw doubts on priority claim(s) or which is cited to establish the publication date of another citation or other special reason (as specified)

"O" document referring to an oral disclosure, use, exhibition or other means

"P" document published prior to the international filing date but later than the priority date claimed

"T" later document published after the international filing date or priority date and not in conflict with the application but cited to understand the principle or theory underlying the invention

"X" document of particular relevance; the claimed invention cannot be considered novel or cannot be considered to involve an inventive step when the document is taken alone

"Y" document of particular relevance; the claimed invention cannot be considered to involve an inventive step when the document is combined with one or more other such documents, such combination being obvious to a person skilled in the art.

"&" document member of the same patent family

Date of the actual completion of the international search	Date of mailing of the international search report
1 April 2004	14/04/2004

Name and mailing address of the ISA	Authorized officer
European Patent Office, P.B. 5818 Patentlaan 2 NL - 2280 HV Rijswijk Tel. (+31-70) 340-2040, Tx. 31 651 epo nl, Fax: (+31-70) 340-3016	Swartjes, H

Form PCT/ISA/210 (second sheet) (January 2004)

INTERNATIONAL SEARCH REPORT

PCT/GB 03/05094

C.(Continuation) DOCUMENTS CONSIDERED TO BE RELEVANT

Category °	Citation of document, with indication, where appropriate, of the relevant passages	Relevant to claim No.
A	US 6 163 155 A (BITTAR MICHAEL S) 19 December 2000 (2000-12-19) column 1, line 91 - line 37	1,12
A	MACGREGOR L ET AL: "Electrical resistivity structure of the Valu Fa Ridge, Lau Basin, from marine controlled-source electromagnetic sounding" GEOPHYSICAL JOURNAL INTERNATIONAL, BLACKWELL SCIENTIFIC PUBLICATIONS, OXFORD, GB, vol. 146, no. 1, July 2001 (2001-07), pages 217-236, XP002234785 ISSN: 0956-540X page 218, right-hand column, last paragraph - page 220, left-hand column, paragraph 1 figure 2	1,12

INTERNATIONAL SEARCH REPORT

PCT/GB 03/05094

Patent document cited in search report	Publication date	Patent family member(s)		Publication date
WO 0120366 A	22-03-2001	AU	768698 B2	08-01-2004
		AU	7129900 A	17-04-2001
		BR	0013969 A	17-09-2002
		CA	2383931 A1	22-03-2001
		CN	1378652 T	06-11-2002
		EP	1218775 A1	03-07-2002
		NO	20021225 A	10-05-2002
		WO	0120366 A1	22-03-2001
		US	6603313 B1	05-08-2003
GB 2382875 A	11-06-2003	WO	03048812 A1	12-06-2003
US 4617518 A	14-10-1986	AU	3571784 A	30-05-1985
		ES	8606671 A1	01-10-1986
		FR	2555322 A1	24-05-1985
		GB	2155182 A	18-09-1985
		JP	60135783 A	19-07-1985
		NL	8403541 A	17-06-1985
		NO	844614 A	22-05-1985
US 6163155 A	19-12-2000	CA	2359371 A1	03-08-2000
		EP	1155343 A1	21-11-2001
		NO	20013707 A	18-09-2001
		WO	0045195 A1	03-08-2000
		US	2003051914 A1	20-03-2003
		US	6476609 B1	05-11-2002
		US	2004027131 A1	12-02-2004